

# Forward-Backward Multiplicity Correlations in pp Collisions at 400 GeV/c

Wang Shaoshun, Zhang Jie, Ye Yunxiu, Xiao Chenguo, Luo Qi, Cheng Zhengdong, Zhang Xueqian, Xu Wanli, and Xiong Weijun

(Department of Modern Physics, University of Science and Technology of China, Hefei, Anhui, China)

The pseudorapidity distributions of charged particles produced in pp collisions at 400 GeV/c have been measured using LEBC films. The multiplicity distributions in forward hemisphere at fixed total multiplicities are obtained. The forward-backward multiplicity correlation strength in full-phase space, central region, and off-central region of the pseudorapidity distribution are calculated. The correlation strength versus pseudorapidity windows are obtained. The experimental data of the forward-backward correlation have been analyzed with cluster model. The results show that the average cluster size is dependent on whether the leading-particle effect is taken into account.

---

## 1. INTRODUCTION

In order to study the production mechanism of the final state high energy hadrons, a topic which has caused wide interests is to study forward-backward hemisphere multiplicity correlations. It provides a very good testing method of various models for hadron production and represents a useful tool for the comparison of different types of collisions.

The experimental results [1,2] show that the forward-backward multiplicity correlation in high energy hadron-hadron collisions increase with increasing CMS energy. If we denote by  $\langle n_B \rangle_{n_F}$ , the average multiplicity in the backward hemisphere when the multiplicity  $n_F$  in the forward hemisphere is fixed, the forward-backward multiplicity correlation can be described by the following formula

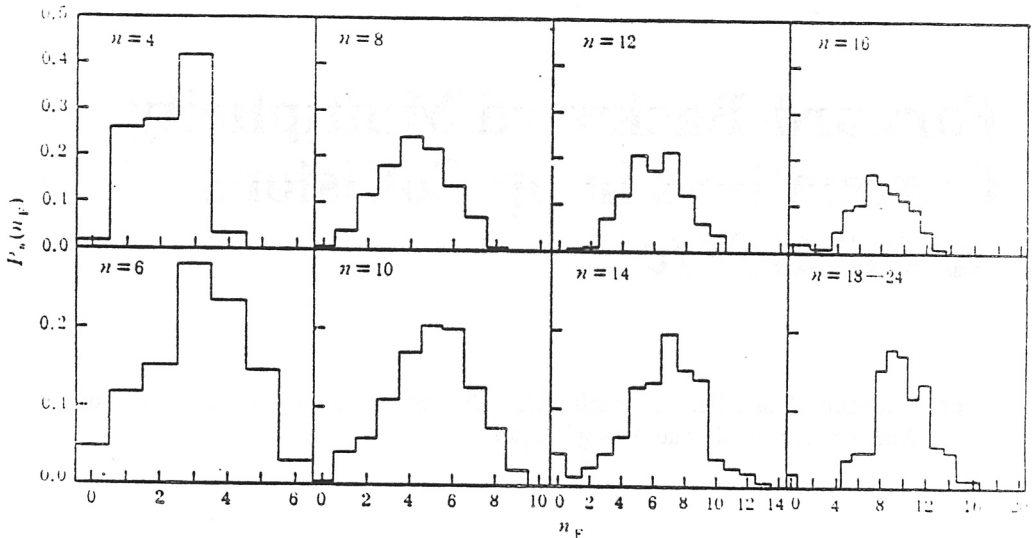


**Fig. 1**  
The multiplicity distributions in the forward hemisphere at fixed total multiplicities.

$$\langle n_B \rangle^{n_F} = a + b n_F, \quad (1)$$

The correlation strength  $b$  is positive over a wide energy range ( $10 \leq \sqrt{S} \leq 900$  GeV) and increases logarithmically with increasing energy. However, this type of correlations in  $e^-e^-$  collisions [3] and lepton-hadron collisions [4] are either unobservable or are very weak. Many theoretical models [5] have been used to explain these correlations. Most of the models [6] based on the final state particles appearing to be group in cluster have assumed that the cluster is neutral and that every cluster decays into two charged particles. The calculated results conform to the experimental results for high energy, but not for low energy. S. L. Lim *et al.* [7] suggested that the average cluster size varies with energy. They obtained better results compared to the experimental data, but they did not consider the leading particle effect, so the obtained average cluster size is notably small at low energy. We have measured the pseudorapidity distributions for charged particles produced in pp collisions at 400 GeV/c by using the LEBC films offered by CERN NA27 collaboration. The forward-backward multiplicity correlations in full-phase space, central region, and off-central region of the pseudorapidity distribution and the correlation strength  $b$  versus pseudorapidity window are calculated. The experimental data have been fitted with cluster model. The better results conforming to the experimental data have been obtained.

## 2. EXPERIMENTAL RESULTS

On the basis of the experimental work [8] of the multiplicity distribution of charged particles produced in pp collisions at 400 GeV/c, the space geometry reconstruction was carried out for the 1798 nonsingle diffractive events with charged multiplicities of 4-24. The pseudorapidity distributions in laboratory system and in center-of-mass system were obtained (see [9] for the measuring method). The multiplicity distributions in the forward hemisphere at fixed total multiplicities thus obtained are shown in Fig. 1.

**Table 1**  
The value of parameters  $a$  and  $b$  at different pseudorapidity ranges.

Pseudorapidity range	$ \eta_c  \geq 0$	$ \eta_c  \leq 1$	$ \eta_c  > 1$
$a$	$3.660 \pm 0.067$	$1.291 \pm 0.047$	$2.861 \pm 0.041$
$b$	$0.221 \pm 0.028$	$0.314 \pm 0.023$	$-0.030 \pm 0.024$

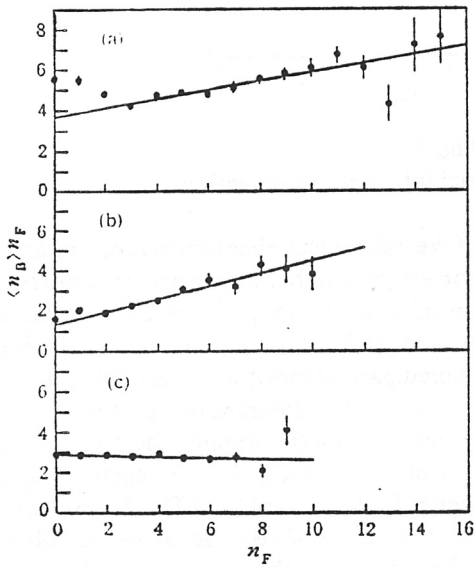


**Fig. 2**

The average backward hemisphere multiplicities versus the forward hemisphere multiplicities. (a) full-phase space ( $|\eta_c| \geq 0$ ); (b) pseudorapidity central range ( $|\eta_c| \leq 1$ ); and (c) pseudorapidity outer central range ( $|\eta_c| > 1$ ). The lines are linear fits to the experimental data.

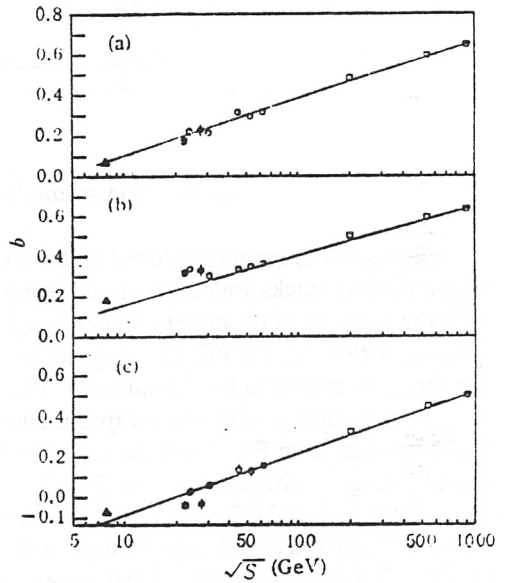


**Fig. 3**

The correlation strength  $b$  versus CMS energy for different pseudorapidity regions. (a) full phase space; (b) pseudorapidity central range; (c) pseudorapidity outer central range.  $\circ$  R701(ISR);  $\square$  UA5;  $\blacksquare$  NA22;  $\blacktriangle$  USSR [10];  $\bullet$  The present experiment.

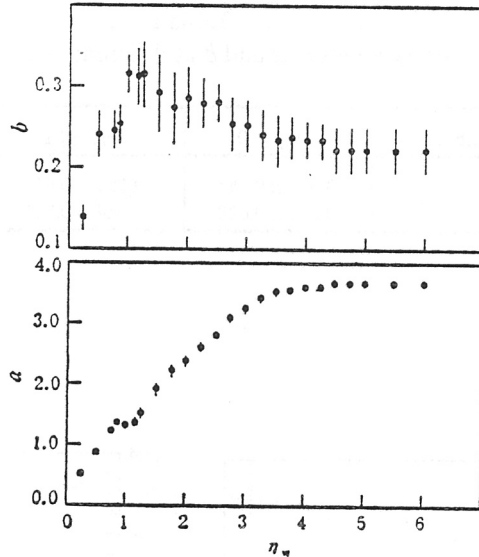


Fig. 4

Correlation strength  $b$  and intercept  $a$  vary with  $\eta_w$ .

Because the events produced at the edge of the bubble chamber fiducial volume and the events with indistinct tracks are not counted, we must correct the number of geometry reconstructive events with the number of observed events [8] and then calculate  $\langle n_B \rangle_{\eta_F}$ . Figure 2 shows the variation of  $\langle n_B \rangle_{\eta_F}$  with  $\eta_F$  for the full-phase space,  $|\eta_C| \leq 1$  and  $|\eta_C| > 1$  regions and these experimental data are fitted according to the formula (1). The obtained parameters  $a$  and  $b$  are listed in Table 1.

A comparison with other experimental results [1,10] at different energies is shown in Fig. 3.<sup>1</sup> It can be seen from Fig. 3 that the experimental points fall on the straight line  $b = d + c \ln S$  for the full-phase space situation, where  $S$  is the square of CMS energy. For the central pseudorapidity range there is a deviation from this law at low energy. It can be seen from Fig. 2 and Table 1 that the forward-backward correlation strength at 400 GeV/c pp collisions is stronger for the full-phase space range and pseudorapidity central range, but for  $|\eta_C| > 1$  there is no correlation within the experimental error.

In order to investigate in which domain of the pseudorapidity space the correlations are concentrated at  $\sqrt{S} = 27.4$  GeV, we select different pseudorapidity window  $\eta_w$  to calculate  $\langle n_B \rangle_{\eta_F}$  and relevant parameters  $a$  and  $b$  when  $|\eta_C| < \eta_w$ . Figure 4 shows  $a$  and  $b$  as functions of  $\eta_w$ . It can be seen from Fig. 4 that the intercept  $a$  grows almost linearly with increasing  $\eta_w$  and reaches a saturation value when  $\eta_w > 3$ . The correlation strength  $b$  first increases with increasing  $\eta_w$  towards a maximum value around  $\eta_w = 1$ , then gradually decreases towards the full phase space values.

### 3. EXPERIMENTAL RESULTS FITTED WITH CLUSTER MODEL

Starting from analyzing the experimental results of the forward-backward correlation, Chou and Yang [11] considered that the charged particle multiplicity distribution could be divided into a

<sup>1</sup> The experimental value for  $\sqrt{S} = 24$  GeV at central pseudorapidity range has been corrected according to [1].



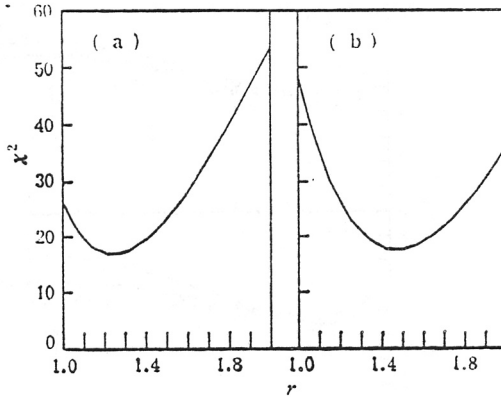


**Fig. 5**

The values of  $\chi^2$  versus fitting parameter  $r$ . (a) leading particle effect included; (b) leading particle effect not included.

stochastic and a non-stochastic part. That is, the numbers of charged particle pairs in the forward and in the backward hemisphere follow a binomial distribution, while the total number  $n = n_F + n_B$  follows the KNO scaling, namely

$$P(n, n_B) = \psi\left(\frac{n}{\bar{n}}\right) C_{n_B/2}^{n/2} \left[ B\left(\frac{n}{2}\right) \right]^{-1}, \tag{2}$$

where  $\psi(n/\bar{n})$  is KNO scaling function,

$$B\left(\frac{n}{2}\right) = \sum_{n_B=0}^n C_{n_B/2}^{n/2}$$

is the normalization factor. S. L. Lim *et al.* made an extension on this basis. They considered that the cluster numbers with average size  $r$  (particle number in a cluster) in the forward and in the backward hemisphere follow binomial distribution, where  $r$  varies with energy, every cluster decaying particles are emitted into the same hemisphere and the leakage effect between the two hemispheres is ignored. Consequently, the distribution of the charged particle's number in the backward hemisphere is

$$P(r, n_B, n) = P(n) C_{n_B/r}^{n/r} \left[ B\left(\frac{n}{r}\right) \right]^{-1}, \tag{3}$$

when  $n$  is fixed. Where  $P(n)$  is the negative binomial distribution which describes the charged particle multiplicity distributions, namely

$$P(n) = \frac{\Gamma(n+k)}{\Gamma(n+1) \cdot \Gamma(k)} \left(\frac{k}{\bar{n}+k}\right)^k \left(\frac{\bar{n}}{\bar{n}+k}\right)^n,$$

here  $k$  is the free parameter,  $\bar{n}$  the average multiplicity. For the 400 GeV/c pp collisions  $\bar{n} = 9.84$ ,  $k = 12.7$  [8]. The normalization factor

$$B\left(\frac{n}{r}\right) = \sum_{n_B=0}^n C_{n_B/r}^{n/r}$$

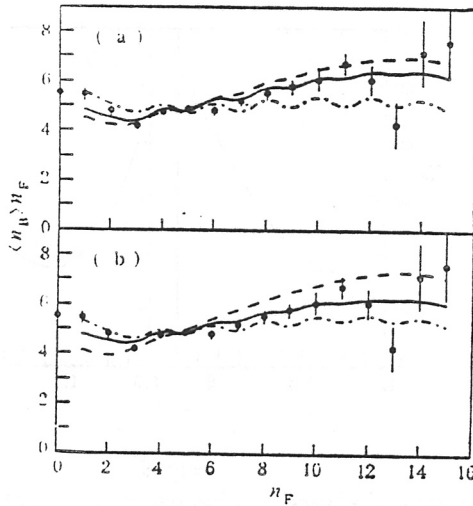


Fig. 6

The experimental results of the forward-backward multiplicity correlations fitted with cluster model for the full-phase space. (a) leading particle effect included; (b) leading particle effect not included.

$r$  = best value; ---  $r = 1$ ; -·-  $r = 2$ .

For the method of calculating the coefficient  $C_{n_B/n}^{n/r}$  see the Appendix. From this we obtain

$$\langle n_B \rangle_{n_F} = \frac{\sum n_B \cdot P(r, n_B, n)}{\sum P(r, n_B, n)}, \quad (4)$$

where

$$\sum = \begin{cases} \sum_{n_B=0,2,4,\dots} & \text{when } n_F = \text{even.} \\ \sum_{n_B=1,3,5,\dots} & \text{when } n_F = \text{odd.} \end{cases}$$

The full phase space experimental data have been fitted using  $\chi^2$  fitting method according to the formula (3) and (4). The values of  $\chi^2$  versus  $r$  are shown in Fig. 5(a). The average cluster size obtained from fitting is  $r = 1.23 \pm 0.09$ . The fitted results are shown in Fig. 6(a), which also shows the fitted curves for  $r = 1$  and 2. Obviously, it conforms to the experimental results very well when  $r = 1.23 \pm 0.09$ . This value is consistent with the calculated results given by S. L. Lim *et al.* (see Fig. 7). But, it is notably small comparing with the average cluster size obtained by other methods [12]. Here an important reason is that the leading-particle effect has not been accounted in the above formula. However, the leading-particle effect plays an important role in pp collisions. In particular, the average multiplicity is small at low energy, so the leading-particle effect cannot be ignored. After taking the leading-particle effect into account, we assume that there is always a final state particle both in the forward and in the backward hemispheres and that other final state particles are distributed binomially in both hemispheres according to the average cluster size. Therefore, formula (3) should be modified to

$$P(r, n_B, n) = P(n) C_{(n, -1)/r}^{(n-2)/r} [B(n/r)]^{-1}, \quad (5)$$

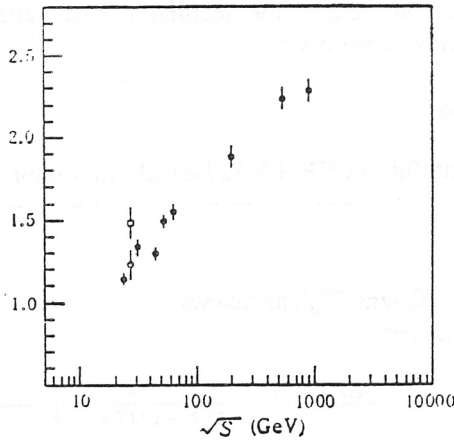


Fig. 7

The average cluster size versus CMS energy. ● the calculated results by S. L. Lim *et al.*; ○ result of the present experiment (leading particle effect included); □ result of the present experiment (leading particle effect not included).

where

$$B(n/r) = \sum_{n_B=1}^{n-1} C_{\langle n_B-1 \rangle / r}$$

correspondingly

$$\langle n_B \rangle_{n_F} = \frac{\sum n_B \cdot P(r, n_B, n)}{\sum P(r, n_B, n)}, \tag{6}$$

where

$$\Sigma = \begin{cases} \sum_{n_B=2,4,\dots} & \text{when } n_F = \text{even.} \\ \sum_{n_B=1,3,\dots} & \text{when } n_F = \text{odd.} \end{cases}$$

The values of  $\chi^2$  versus fitting parameter  $r$  obtained by the same method are shown in Fig. 5(b). Thus, the average cluster size obtained is  $r = 1.47 \pm 0.10$ . The fitted curves for  $r = 1, 2$  and the best value are shown in Fig. 6(b). It conforms to the experimental data better when  $r = 1.47 \pm 0.10$  which can be seen from the figure.

#### 4. RESULTS AND DISCUSSIONS

1) There are clear forward-backward correlations in the full pseudorapidity space and central pseudorapidity range. For the off-central range, namely  $|\eta_c| > 1$ , there is no forward-backward correlation within the experimental error for the 400 GeV/c pp collisions.

2) For the full pseudorapidity space the forward-backward correlation strength  $b$  versus CMS energy satisfied linear relationship  $b = d + c \ln(S)$ .

3) Within a small central range  $|\eta_c| < \eta_w$ , the correlation strength  $b$  increases with increasing  $\eta_w$  towards a maximum value around  $\eta_w = 1$ , then decreases towards the full-phase space value.

4) The experimental data of the forward-backward correlations can be used to determine the average cluster size. At low energy, the leading particle effect should be considered in the determination of the average cluster size.

### ACKNOWLEDGMENTS

The authors are grateful to CERN NA27 collaboration for offering the LEBC films.

### APPENDIX

We calculate the coefficient  $C_{n_B/r}^{n/r}$  as follows:

Let  $n/r = a$ ,  $n_B/r = b$ , namely

$$C_{n_B/r}^{n/r} = C_b^a = \frac{\Gamma(a+1)}{\Gamma(b+1)\Gamma(a-b+1)},$$

when  $a$  and  $b$  are not integers,

$$\Gamma(a) = \sqrt{2\pi} a^{a-1/2} e^{-a} (c_0 + c_1 + c_2 + c_3 + \dots),$$

where  $c_0 = 1$ ,  $c_1 = a^{-1}/12$ ,  $c_2 = a^{-2}/288$ ,  $c_3 = -(139a^{-3}/51840)$ , ...

### REFERENCES

- [1] S. Uhlig *et al.*, *Nucl. Phys.*, **B132** (1978), p. 15.
- [2] R. Ansorge *et al.*, *Z. Phys. C-Particles and Fields*, **37** (1989), p. 191; G. J. Alner *et al.*, *Nucl. Phys.*, **B291** (1987), p. 445; K. Alpgard *et al.*, *Phys. Lett.*, **123B** (1983), p. 361.
- [3] M. Althoff *et al.*, *Z. Phys. C-Particles and Fields*, **29** (1985), p. 347; M. Derrick *et al.*, *Phys. Rev.*, **D34** (1986), p. 3304; W. Braunschweig *et al.*, *Z. Phys. C-Particles and Fields*, **45** (1989), p. 193.
- [4] M. Arneodo *et al.*, *Nucl. Phys.*, **B258** (1985), p. 249.
- [5] A. Capella and J. Tran Thanh Van, *Z. Phys. C-Particles and Fields*, **18** (1983), p. 85; K. Fialkowski *et al.*, *Phys. Lett.*, **115B** (1982), p. 425; J. Kuhn, *Nucl. Phys.*, **B140** (1978), p. 179; S. Barshay, *Z. Phys. C-Particles and Fields*, **32** (1986), p. 513; V. V. Lugovoi and V. M. Chudakov, *Sov. J. Nucl. Phys.*, **50** (1989), p. 490; F. W. Bopp *et al.*, *Z. Phys. C-Particles and Fields*, **51** (1991), p. 99.
- [6] P. Carruthers and C. C. Shih, *Phys. Lett.*, **165B** (1985), p. 209; Cai Xu *et al.*, *Phys. Rev.*, **D33** (1986) 1287; M. Biyajima *et al.*, *Z. Phys. C-Particles and Fields*, **44** (1989), p. 199; M. Biyajima *et al.*, *Phys. Rev.*, **D39** (1989), p. 203.
- [7] S. L. Lim *et al.*, *Z. Phys. C-Particles and Fields*, **43** (1989), p. 621.
- [8] Wang Shaoshun *et al.*, *High Energy Phys. and Nucl. Phys.* (in Chinese), **13** (1989), p. 673.
- [9] Wang Shaoshun *et al.*, *High Energy Phys. and Nucl. Phys.* (in Chinese), **15** (1991), p. 1057.
- [10] V. V. Avivazyan *et al.*, *Z. Phys. C-Particles and Fields*, **42** (1989), p. 533; L. V. Bravina *et al.*, *Sov. J. Nucl. Phys.*, **50** (1989), p. 245.
- [11] T. T. Chou and C. N. Yang, *Phys. Lett.*, **135B** (1984), p. 175.
- [12] Wang Shaoshun *et al.*, *High Energy Phys. and Nucl. Phys.* (in Chinese), **16** (1992), p. 488.